

# Test-Time Generative Augmentation for Medical Image Segmentation

Xiao Ma<sup>1</sup>, Yuhui Tao<sup>1</sup>, Yuhan Zhang<sup>2</sup>, Zexuan Ji<sup>1</sup>, Yizhe Zhang<sup>1</sup> (✉), and Qiang Chen<sup>1</sup> (✉)

<sup>1</sup> School of Computer Science and Engineering, Nanjing University of Science and Technology, Nanjing, China

yizhe.zhang.cs@gmail.com; chen2qiang@njjust.edu.cn

<sup>2</sup> Department of Computer Science and Engineering, The Chinese University of Hong Kong, Hong Kong, China

**Abstract.** In this paper, we propose a novel approach to enhance medical image segmentation during test time. Instead of employing handcrafted transforms or functions on the input test image to create multiple views for test-time augmentation, we advocate for the utilization of an advanced domain-fine-tuned generative model (GM), e.g., stable diffusion (SD), for test-time augmentation. Given that the GM has been trained to comprehend and encapsulate comprehensive domain data knowledge, it is superior than segmentation models in terms of representing the data characteristics and distribution. Hence, by integrating the GM into test-time augmentation, we can effectively generate multiple views of a given test sample, aligning with the content and appearance characteristics of the sample and the related local data distribution. This approach renders the augmentation process more adaptable and resilient compared to conventional handcrafted transforms. Comprehensive experiments conducted across three medical image segmentation tasks (nine datasets) demonstrate the efficacy and versatility of the proposed TTGA in enhancing segmentation outcomes. Moreover, TTGA significantly improves pixel-wise error estimation, thereby facilitating the deployment of a more reliable segmentation system. Code will be released at: <https://github.com/maxiao0234/TTGA>.

**Keywords:** Test-Time Augmentation · Generative Model · Stable Diffusion · Medical Image Segmentation · error estimation.

## 1 Introduction

Deep learning, with its significant advantages in high automation and accuracy, has achieved remarkable success in the field of medical image segmentation [6, 19, 23, 27]. End-to-end segmentation models, which transform input images into binary masks for each class, are extensively employed in medical image analysis. Most previous efforts focused on designing model architectures (e.g., UNet [26], Ds-TransUnet [18]), data utilization (e.g., semi-supervised [14],

weakly-supervised learning [31]), and training methods (e.g., knowledge distillation [24]) to advance medical image segmentation, yet fewer attempts were made in improving segmentation via developing novel test-time methods.

During test time, the actual test sample distribution is accessible (although partially), presenting great opportunities to further improve an already well-trained state-of-the-art segmentation model when processing through these test samples. Previous studies for test-time improvement of segmentation can be categorized into two main approaches: (1) test-time augmentation (e.g., [4]), which involves augmenting test samples using pre-defined transforms and functions to create multiple versions of segmentation for error estimation and/or segmentation ensemble, and (2) test-time model adaptation (e.g., [34]), which entails updating segmentation model parameters with newly seen test samples.

In this paper, we propose a novel method that *generatively* augments test data during test time to improve segmentation error estimation as well as segmentation accuracy. The augmentation operates at the per-sample level: given a test image, we utilize a stable diffusion model (DM) to generate a set of new samples that are closely related to the current test sample but with varying appearances. We then apply the segmentation model (under testing) to the generated samples to obtain a set of segmentation maps. By combining the segmentation maps, we can generate a new segmentation map that gives better segmentation quality than the original segmentation map. Moreover, the generated additional segmentations can help generate a pixel-wise error estimation map, informing potential segmentation errors. Our contributions can be summarized in three aspects.

- We proposed test-time generative augmentation (TTGA), which integrates the content of the test sample with the knowledge derived from a generative model trained on medical datasets. This approach generates locally randomized edits to produce realistic images, thereby providing segmentation models with augmented samples closely resembling the in-domain knowledge.
- We developed a novel diffusion inversion approach termed masked null-text inversion. During the denoising process, the noise predicted using embeddings containing image information as conditional predictors is substituted with the noise predicted without image information within randomly generated mask regions. This modification aims to alter the content of the image within the masked regions.
- We conducted comprehensive experiments on the proposed test-time generative augmentation using three medical image segmentation tasks and validated TTGA’s effectiveness in generating better segmentation results and error estimation.

## 2 Related Work

**Test-time Augmentation.** Our method is a novel type of test-time augmentation (TTA) method. In this section, we give an overview of the existing TTA

methods, highlighting the advantages and novel aspects of the proposed method against them. The process of TTA typically involves applying transformations such as flipping, rotation, scaling, cropping, or color jittering to the test images before feeding them into the model for inference. By considering multiple views of the same test instance, TTA generates better segmentation output by ensemble or fusing segmentation from the multi-views [22, 30]. In addition, the variances among the segmentation of the views can be used for pixel-wise error estimation [4, 29]. Existing TTA methods either rely on generic geometric transforms to create multiple views or rely on designing specific transforms/functions for particular segmentation tasks/models. Our proposed generative augmentation (TTGA) is generally applicable to a wide range of medical image segmentation tasks/datasets and is agnostic to the segmentation model used. The proposed TTGA, via utilizing a state-of-the-art generative model, can create new views of a test sample based on the image content and data distribution, superior to hand-crafted transforms and functions.

**Sample Generation.** Generative models have garnered significant attention owing to their exceptional realism and diversity [10, 25, 32]. As a form of image-to-image translation, image editing enables targeted modifications to specific content within an image while maintaining consistency with the remaining content [13]. Limited by the lack of accompanying textual data and the difficulties associated with employing text-driven control methods, region-based control emerges as a more feasible approach for medical data. In this study, we devised a novel image augmentation strategy tailored for medical images through diffusion inversion. Specifically, this entails augmenting randomly masked regions within the test image while preserving content consistency in the non-masked areas.

### 3 Method

#### 3.1 Background

Diffusion probabilistic model (DPM) is a recently popularized framework in generative modeling, utilized to simulate the data generation process. Taking denoising diffusion probabilistic model (DDPM) [10] as an example, given an initial real image  $x_0$ , the forward diffusion process undergoes  $T$  steps of a Markovian noise addition process, producing a noise image  $x_T$  that conforms to a standard Gaussian distribution  $\mathcal{N}(0, I)$ . For a well-trained DM  $\mu_\theta$ , starting from the noisy image  $\tilde{x}_T$ , the process progressively denoises to recover a simulated image  $\tilde{x}_0$  representative of the distribution of the training dataset. The forward and reverse steps can be expressed as:

$$q(x_t|x_{t-1}) := \mathcal{N}(x_t; \sqrt{\alpha_t}x_{t-1}, (1 - \alpha_t)I) \quad (1)$$

$$p_\theta(x_{t-1}|x_t) := \mathcal{N}(x_{t-1}; \mu_\theta(x_t, t), \Sigma_\theta) \quad (2)$$

where  $\{\alpha_t\}_{t=1}^T$  is the a series of predetermined hyper-parameters and the  $\Sigma_\theta$  is a fixed variance. Denoising diffusion implicit model (DDIM) [28] generalizes

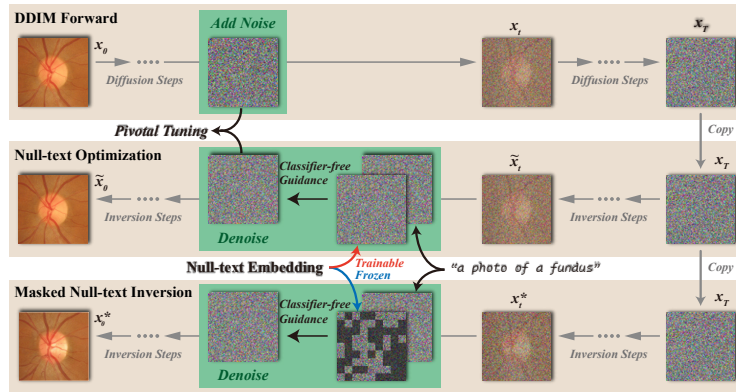


**Fig. 1.** The pipelines of DDIM forward, null-text inversion, and our masked null-text inversion are presented. The trainable null-text embedding is optimized in a single inversion, which can generate an image approximating the initial one. After adding masks to the noise predicted by null-text embedding, the generated image undergoes localized variances.

the inversion steps of DDPM through a class of non-Markovian deterministic generation, enhancing both the generation speed and quality.

In order to acquire generated images that meet the requirements, conditional DMs utilize the image and condition pairs for training. During the inference process, the requisite conditions are adopted as guidance for the denoising steps. Classifier-free guidance [11] is a widely adopted conditional guiding generative paradigm. The noise prediction step is described as the combination of a unconditional and a conditional predictions:

$$\tilde{\epsilon}_t = \epsilon_\theta(x_t, t, \emptyset) + \omega \cdot (\epsilon_\theta(x_t, t, c) - \epsilon_\theta(x_t, t, \emptyset)) \quad (3)$$

where the  $\emptyset$  is the unconditional embedding, the  $c$  is the conditional embedding and the  $\omega$  is the guidance scale.

### 3.2 Masked Null-Text Inversion

Although the image-to-image DDIM inversion process with classifier-free guidance is capable of generating new images that conform to the guidance conditions, the editability of this method is extremely limited. The content of the images is typically subject to substantial random modifications. To ensure consistency between the non-editing areas and the initial image during the image editing process, some methods tune conditional [7] or unconditional [21] embeddings. These approaches help preserve the more original content of the image during the prediction process guided with new information. However, for medical images, datasets with detailed conditions are scarce. Typically, only a limited amount of category information is available, which necessitates the need for image editing methods that have a weaker dependency on conditions. As depicted

in Fig. 1, we propose an image editing method called masked null text inversion, which implements random modifications to localized areas.

The vanilla null-text inversion learns a new set of null-text embeddings during the DDIM inversion process [21]. This makes the noise predicted at each inversion step approximate the forward-added noise, ultimately generating images that maintain a high level of consistency with the original ones. Specifically, pivotal tuning is executed sequentially from step  $T$  to step  $0$ :

$$\mathcal{L}_t = \|x_{t-1} - \tilde{x}_{t-1}(\tilde{x}_t, \tilde{\mathcal{D}}_t, c)\|_2^2 \quad (4)$$

where only the null-text embedding  $\tilde{\mathcal{D}}_t$  is updated in the optimization at the step  $t$ . When the conditional embeddings  $c$  remain unchanged, the use of this tuned set of null-text embeddings  $E = \{\tilde{\mathcal{D}}_t\}_{t=1}^T$  as unconditional ones results in a generated image  $\tilde{x}_0$  that is nearly identical to the original image  $x_0$ .

Building on this, we aim to generate realistic images with localized changes based on the original image without relying on modifications to the conditional embeddings. As illustrated in Fig. 1, at the start of a new round of inversion, we randomly initialize a mask  $m \sim \mathcal{B}(s_m, p_m)$  that follows a Bernoulli distribution, where  $s_m$  is the size of  $x_t$  and  $p_m$  represents the probability of the mask. During the selected steps  $\{\tau\} \subset \{t\}$ , the classifier-free guidance noise prediction within the mask area is discarded:

$$\epsilon_\tau^* = \omega \cdot \epsilon_\theta(x_\tau^*, \tau, c) + (1 - \omega) \cdot ((1 - m) \cdot \epsilon_\theta(x_\tau^*, \tau, \tilde{\mathcal{D}}_\tau) + m \cdot \epsilon_\tau^\spadesuit) \quad (5)$$

where the  $\epsilon_\tau^\spadesuit$  denotes the externally introduced noise with a similar conditional distribution as the  $\tilde{\mathcal{D}}_t$  guided noise. To simplify, we recommend using the unconditional noise prediction from the same step guided by the same conditional embedding in another round:

$$\epsilon_\tau^\spadesuit = \epsilon_\theta(\tilde{y}_\tau, \tau, \emptyset) \quad (6)$$

where the  $\tilde{y}_\tau$  refers to the denoised sample at the  $t$  step, predicted from the initial noise at  $y_T$ . In each prediction of the selected steps, the unconditional noise within the mask is altered, while the information of the initial image is maintained outside the region under the guidance of  $\tilde{\mathcal{D}}_\tau$ . The general classifier-free noise prediction retains the guidance of  $c$ . Consequently, this ensures that the overall content of the final generated image remains unchanged, with local random modifications occurring within and near the mask area.

### 3.3 Test-Time Generative Augmentation

We further introduce test-time generative augmentation (TTGA), building on our generative scheme. Given a test image  $x$ , a set of null-text embeddings  $E'$  is obtained through one round of null-text optimization. Subsequently,  $N$  masks are generated and applied through  $N$  rounds of masked null-text inversion, resulting in a set of generative augmented images. A segmentation model

performs multiple segmentations on the augmented images, and an ensemble of these segmentation results is used to obtain a posterior regarding the test image:

$$p(x') = \frac{1}{N} \cdot \sum_{i=1}^N p(f(x', m'_i, E')) \quad (7)$$

where the  $f(\cdot)$  the execution of a masked null-text inversion. With regard to the ensemble results, their uncertainty  $H$  can be further estimated. In this work, we employ entropy as a measure of uncertainty:

$$H(p) = \sum_{k=1}^K p_k \cdot \log_2(p_k) \quad (8)$$

where the  $K$  is the quantity of different classes.

For the generalizability of the masked null-text inversion in TTGA, the latent DMs remain practical. The latent feature of a test image is edited through diffusion steps and a set of augmented images is decoded from the augmented features. In this work, we utilize pre-trained stable diffusion v1-5 [25] as the backbone of our DM.

## 4 Experiments

### 4.1 Materials

We evaluate our TTGA in three medical image segmentation tasks. Serving as a general method for improving segmentation and error estimation, we choose a state-of-the-art (SOTA) segmentation model with open-source parameters for each task to conduct experiments.

**Optic Disc and Cup Segmentation:** We first employ the REFUGE2 dataset to evaluate the proposed method on segmentation of optic discs and cups in images acquired by fundus cameras. We employ a SOTA Transformer-based segmentation model [16], with utilization of the well-trained model weights and codes published at [1].

**Polyp Segmentation:** We extend our evaluation to include polyp segmentation in endoscopic images. We employ HSNNet [33] as our segmentation model, utilizing the codes and weights published at [2]. The model was trained using a subset of images from the Kvasir and CVC-ClinicDB datasets. As per Zhang et al. [33], the test set was curated using the remaining samples from Kvasir and CVC-ClinicDB (“seen” part), along with samples from three additional datasets (“unseen” part): CVC-ColonDB, CVC-300, and ETIS-LiaribPolypDB.

**Skin Lesion Segmentation:** We investigate the effectiveness of the proposed method in skin lesion segmentation. For this task, we utilize a SOTA segmentation model for skin lesion segmentation [5], which underwent training utilizing the ISIC 2017 training set. We use the well trained model and the related codes

published by the authors [3]. Subsequently, we evaluate the segmentation performance on the test sets of ISIC 2017 and ISIC 2018 (“seen” part), and PH2 (“unseen” part).

For each segmentation task, before performing the inversion, we tune our DM using the same training data used for training the segmentation model with a fixed text condition. This ensures that the DM has knowledge of the specific image content of the field. Besides, we set the total number of DDIM sampling steps to 20 and apply the masking strategy to the noise in the final 5 steps.

For a fair comparison, we employ two general test-time strategies that are not confined to any specific type of data or model. **Test-time Dropout (TTD)** generates perturbed model outputs by randomly dropping certain layers. We employ Monte Carlo (MC) [8] dropout as the implementation scheme for TTD. **Test-time Augmentation (TTA)** perturbed data outputs by applying variances to the input image. We use a combination of multi-view [22] and morphological transformations [4] as our comparative methods. All strategies combine ten different segmentation results obtained from a single test image. We evaluate the results in two aspects: pixel-wise error estimation (Sec. 4.2) and segmentation accuracy (Sec. 4.3). Both evaluations utilize the **Dice Similarity Coefficient (DSC)** and **Area Under the Curve (AUC)** measures.

#### 4.2 On Improving Pixel-wise Error Estimation

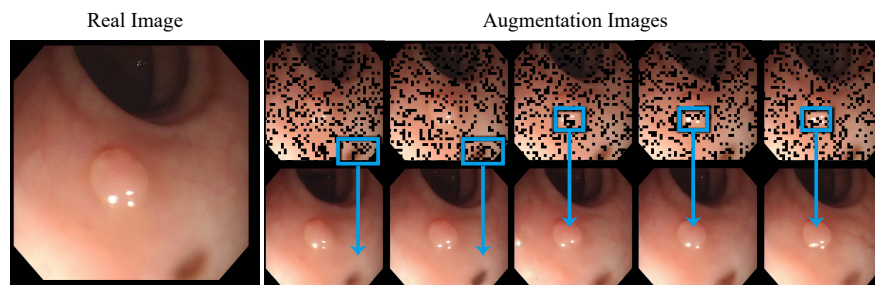


**Fig. 2.** Visualization of Augmentation Results. During the diffusion inversion process, random masks are applied. The generated images exhibit a high level of consistency with the real images. Significant changes occur in the masked areas, effectively achieving the desired augmentation effect.

In this section, we describe the experimental results of the error estimation (error estimation) of the network segmentation results using our proposed method. We consider the difference area between the network segmentation results of the test images and the ground truths as the pixel-wise error areas. A uncertainty score per-pixel is calculated based on Eq. 8 for the assessment results during the test-time, which is then validated against the pixel-wise error

**Table 1.** Individual and combination performance of pixel-wise error estimation on REFUGE2. The ‘All’ refers to the combination of TTD, TTA and TTGA.

	TTD [8]	TTA [4, 22]	TTD+TTA	TTGA	TTD+TTGA	All
DSC(Disc)	0.4522	0.4482	0.4574	<b>0.4760</b>	0.4753	0.4745
AUC(Disc)	0.9814	0.9842	0.9849	<b>0.9872</b>	0.9863	0.9868
DSC(Cup)	0.5061	0.4891	0.5068	<b>0.5188</b>	0.5145	0.5187
AUC(Cup)	0.9870	0.9854	0.9898	0.9906	0.9907	<b>0.9911</b>

**Table 2.** Pixel-wise error estimation on three tasks.

Method		Fundus	Polyp		Skin	
		REFUGE2	“seen”	“unseen”	“seen”	“unseen”
TTD [8]	DSC	0.4792	0.4100	0.4066	0.3413	0.4273
	AUC	0.9846	0.9042	0.8949	0.8621	0.9044
TTA [4, 22]	DSC	0.4821	0.3811	0.4106	0.3621	0.4260
	AUC	0.9874	0.9333	0.9267	0.8832	0.9091
TTGA(Ours)	DSC	<b>0.4974</b>	<b>0.4164</b>	<b>0.4297</b>	<b>0.3783</b>	<b>0.4316</b>
	AUC	<b>0.9889</b>	<b>0.9461</b>	<b>0.9401</b>	<b>0.8952</b>	<b>0.9178</b>

area. We first analyze the performance and the combination performance of our method and the comparative methods on REFUGE2. Tab. 1 demonstrates the performance of various strategy combinations. Our TTGA exceeds TTD and TTA by 0.0238 and 0.0278 in dice measure respectively on error estimation for the optic disc, and by 0.0127 and 0.0297 in dice measure respectively for the error estimation on the optic cup. TTD introduces uncertainty regarding the model parameters, while TTA introduces uncertainty about the data. These two can supplement each other, hence the performance of TTD and TTA combined is higher than when they are applied individually. Our method shows almost no decline in performance when superimposing results with a lower numerical value, indicating robustness in our error estimation. Additionally, our method also serves as a form of data augmentation. In subsequent experimental results, to showcase better effectiveness, we superimpose the results of TTD on both TTA and our TTGA.

To further discuss the modeling capability in error estimation, we evaluated the comparison results on additional datasets. Tab. 2 presents the performance across three datasets. Our approach demonstrates superior average performance across various tasks compared to the baseline methods. Particularly, on datasets not included in the training set, our results exhibit a competitive advantage over other methods, which may be attributed to the generative image augmentation strategy that possesses certain image domain generalization capabilities. More qualitative augmentation results are shown in Fig. 2

### 4.3 On Improving Segmentation Accuracy

We evaluate the performance of segmentation following the ensemble of individual segmentation outcomes on Tab. 3. We find that the use of TTD might have a negative impact on the final segmentation performance. Two schemes for aug-



**Table 3.** Segmentation results on three tasks.

Method		Fundus	Polyp		Skin	
		REFUGE2	"seen"	"unseen"	"seen"	"unseen"
Vanilla	DSC	0.8863	<b>0.9397</b>	0.8432	0.8342	0.8973
	AUC	0.9957	0.9725	0.9460	0.9690	0.9836
TTD [8]	DSC	0.8975	0.9343	0.8292	0.8394	0.9010
	AUC	0.9979	0.9885	0.9707	0.9687	0.9812
TTA [4, 22]	DSC	0.8973	0.9390	0.8439	<b>0.8449</b>	0.9031
	AUC	0.9982	<b>0.9912</b>	<b>0.9787</b>	0.9629	<b>0.9894</b>
TTGA(Ours)	DSC	<b>0.9021</b>	0.9394	<b>0.8481</b>	0.8446	<b>0.9078</b>
	AUC	<b>0.9986</b>	0.9908	0.9761	<b>0.9782</b>	0.9884

menting images, namely TTA and our proposed TTGA, showed improvement over the original network output. This suggests that the image segmentation network exhibits a strong dependency on image information. Although the overall segmentation performance of our proposed TTGA and TTA are comparable, when combined with error estimation, the generative image augmentation scheme demonstrates to be a more promising approach.

## 5 Conclusion

In this paper, we developed a novel method (TTGA) for test-time augmentation by leveraging an advanced generative model, stable diffusion, to achieve content-based augmentation for improving medical image segmentation. Our method is effective, robust, and flexible, suggesting a promising direction in applying test-time generative process in enhancing medical image segmentation.

## Bibliography

- [1] Official Code of Segmentation Model used in Optic Disc and Cup Segmentation. <https://github.com/askerlee/segtran/>
- [2] Official Code of Segmentation Model used in Polyp Segmentation. <https://github.com/baiboat/HSNet/>
- [3] Official Code of Segmentation Model used in Skin Lesion Segmentation. <https://github.com/rezazad68/TMUnet/>
- [4] Ayhan, M.S., Berens, P.: Test-time data augmentation for estimation of heteroscedastic aleatoric uncertainty in deep neural networks. In: MIDL (2022)
- [5] Azad, R., Heidari, M., Wu, Y., Merhof, D.: Contextual attention network: Transformer meets u-net. In: International Workshop on Machine Learning in Medical Imaging. pp. 377–386. Springer (2022)
- [6] Bateson, M., Kervadec, H., Dolz, J., Lombaert, H., Ayed, I.B.: Source-free domain adaptation for image segmentation. *Medical Image Analysis* **82**, 102617 (2022)
- [7] Dong, W., Xue, S., Duan, X., Han, S.: Prompt tuning inversion for text-driven image editing using diffusion models. arXiv preprint [arXiv:2305.04441](https://arxiv.org/abs/2305.04441) (2023)
- [8] Gal, Y., Ghahramani, Z.: Dropout as a bayesian approximation: Representing model uncertainty in deep learning. In: international conference on machine learning. pp. 1050–1059. PMLR (2016)
- [9] Gawlikowski, J., Tassi, C.R.N., Ali, M., Lee, J., Humt, M., Feng, J., Kruspe, A., Triebel, R., Jung, P., Roscher, R., et al.: A survey of uncertainty in deep neural networks. *Artificial Intelligence Review* **56**(Suppl 1), 1513–1589 (2023)
- [10] Ho, J., Jain, A., Abbeel, P.: Denoising diffusion probabilistic models. *Advances in neural information processing systems* **33**, 6840–6851 (2020)
- [11] Ho, J., Salimans, T.: Classifier-free diffusion guidance. arXiv preprint [arXiv:2207.12598](https://arxiv.org/abs/2207.12598) (2022)
- [12] Hu, Q., Chen, Y., Xiao, J., Sun, S., Chen, J., Yuille, A.L., Zhou, Z.: Label-free liver tumor segmentation. In: Proceedings of the IEEE/CVF Conference on Computer Vision and Pattern Recognition. pp. 7422–7432 (2023)
- [13] Huang, Y., Huang, J., Liu, Y., Yan, M., Lv, J., Liu, J., Xiong, W., Zhang, H., Chen, S., Cao, L.: Diffusion model-based image editing: A survey. arXiv preprint [arXiv:2402.17525](https://arxiv.org/abs/2402.17525) (2024)
- [14] Jiao, R., Zhang, Y., Ding, L., Xue, B., Zhang, J., Cai, R., Jin, C.: Learning with limited annotations: a survey on deep semi-supervised learning for medical image segmentation. *Computers in Biology and Medicine* p. 107840 (2023)
- [15] Jungo, A., Reyes, M.: Assessing reliability and challenges of uncertainty estimations for medical image segmentation. In: MICCAI. pp. 48–56. Springer (2019)

- [16] Li, S., Sui, X., Luo, X., Xu, X., Liu, Y., Goh, R.: Medical image segmentation using squeeze-and-expansion transformers. arXiv preprint [arXiv:2105.09511](https://arxiv.org/abs/2105.09511) (2021)
- [17] Li, Z., Kamnitsas, K., Dou, Q., Qin, C., Glocker, B.: Joint optimization of class-specific training-and test-time data augmentation in segmentation. *IEEE-TMI* (2023)
- [18] Lin, A., Chen, B., Xu, J., Zhang, Z., Lu, G., Zhang, D.: Ds-transunet: Dual swin transformer u-net for medical image segmentation. *IEEE Transactions on Instrumentation and Measurement* **71**, 1–15 (2022)
- [19] Ma, X., Ji, Z., Niu, S., Leng, T., Rubin, D.L., Chen, Q.: Ms-cam: Multi-scale class activation maps for weakly-supervised segmentation of geographic atrophy lesions in sd-oct images. *IEEE Journal of Biomedical and Health Informatics* **24**(12), 3443–3455 (2020)
- [20] Mehrtash, A., Wells, W.M., Tempany, C.M., Abolmaesumi, P., Kapur, T.: Confidence calibration and predictive uncertainty estimation for deep medical image segmentation. *IEEE-TMI* **39**(12), 3868–3878 (2020)
- [21] Mokady, R., Hertz, A., Aberman, K., Pritch, Y., Cohen-Or, D.: Null-text inversion for editing real images using guided diffusion models. In: *Proceedings of the IEEE/CVF Conference on Computer Vision and Pattern Recognition*. pp. 6038–6047 (2023)
- [22] Moshkov, N., Mathe, B., Kertesz-Farkas, A., Hollandi, R., Horvath, P.: Test-time augmentation for deep learning-based cell segmentation on microscopy images. *Scientific reports* **10**(1), 5068 (2020)
- [23] Özbey, M., Dalmaz, O., Dar, S.U., Bedel, H.A., Öztürk, Ş., Güngör, A., Çukur, T.: Unsupervised medical image translation with adversarial diffusion models. *IEEE-TMI* (2023)
- [24] Qin, D., Bu, J.J., Liu, Z., Shen, X., Zhou, S., Gu, J.J., Wang, Z.H., Wu, L., Dai, H.F.: Efficient medical image segmentation based on knowledge distillation. *IEEE-TMI* **40**(12), 3820–3831 (2021)
- [25] Rombach, R., Blattmann, A., Lorenz, D., Esser, P., Ommer, B.: High-resolution image synthesis with latent diffusion models. In: *Proceedings of the IEEE/CVF conference on computer vision and pattern recognition*. pp. 10684–10695 (2022)
- [26] Ronneberger, O., Fischer, P., Brox, T.: U-net: Convolutional networks for biomedical image segmentation. In: *MICCAI*. pp. 234–241. Springer (2015)
- [27] Roy, S., Koehler, G., Ulrich, C., Baumgartner, M., Petersen, J., Isensee, F., Jaeger, P.F., Maier-Hein, K.H.: Mednext: transformer-driven scaling of convnets for medical image segmentation. In: *MICCAI*. pp. 405–415. Springer (2023)
- [28] Song, J., Meng, C., Ermon, S.: Denoising diffusion implicit models. arXiv preprint [arXiv:2010.02502](https://arxiv.org/abs/2010.02502) (2020)
- [29] Wang, G., Li, W., Aertsen, M., Deprest, J., Ourselin, S., Vercauteren, T.: Aleatoric uncertainty estimation with test-time augmentation for medical image segmentation with convolutional neural networks. *Neurocomputing* **338**, 34–45 (2019)

- [30] Wang, G., Li, W., Ourselin, S., Vercauteren, T.: Automatic brain tumor segmentation using convolutional neural networks with test-time augmentation. In: *Brainlesion*. pp. 61–72. Springer (2019)
- [31] Xu, G., Song, Z., Sun, Z., Ku, C., Yang, Z., Liu, C., Wang, S., Ma, J., Xu, W.: Camel: A weakly supervised learning framework for histopathology image segmentation. In: *Proceedings of the IEEE/CVF International Conference on computer vision*. pp. 10682–10691 (2019)
- [32] Zhang, L., Rao, A., Agrawala, M.: Adding conditional control to text-to-image diffusion models. In: *Proceedings of the IEEE/CVF International Conference on Computer Vision*. pp. 3836–3847 (2023)
- [33] Zhang, W., Fu, C., Zheng, Y., Zhang, F., Zhao, Y., Sham, C.W.: Hsnet: A hybrid semantic network for polyp segmentation. *Computers in biology and medicine* **150**, 106173 (2022)
- [34] Zhang, Y., Zhou, T., Tao, Y., Wang, S., Wu, Y., Liu, B., Gu, P., Chen, Q., Chen, D.Z.: Testfit: A plug-and-play one-pass test time method for medical image segmentation. *Medical Image Analysis* **92**, 103069 (2024)
- [35] Zheng, H., Zhang, Y., Yang, L., Liang, P., Zhao, Z., Wang, C., Chen, D.Z.: A new ensemble learning framework for 3d biomedical image segmentation. In: *AAAI*. vol. 33, pp. 5909–5916 (2019)
- [36] Zhou, L.: Spatially exclusive pasting: A general data augmentation for the polyp segmentation. In: *2023 International Joint Conference on Neural Networks (IJCNN)*. pp. 01–07. IEEE (2023)